

Superconductivity in amorphous and crystalline Re-Lu films

Serafim Teknowijoyo and Armen Gulian*

*Advanced Physics Laboratory, Institute for Quantum Studies,
Chapman University, Burtonsville, MD 20866, USA*

We report on magnetron deposition and superconducting properties of a novel superconducting material: rhenium-lutetium films on sapphire substrates. Different compositions of Re_xLu binary are explored from $x \approx 3.8$ to close to pure Re stoichiometry. The highest critical temperature, up to $T_c \approx 6.95$ K, is obtained for $x \approx 10.5$. Depending on the deposition conditions, polycrystalline or amorphous films are obtainable, both of which are interesting for practice. Crystalline structure of polycrystalline phase is identified using grazing incidence X-ray diffractometry as a non-centrosymmetric superconductor. Superconducting properties were characterized both resistively and magnetically. Demonstration of superconductivity in this material justifies the point of view that Lu plays a role of group 3 transition metal in period 6 of the Periodic table of elements. In analogy with $\text{Re}_{0.82}\text{Nb}_{0.18}$, Re_6Ti , Re_6Hf and Re_6Zr , one can expect that crystalline Re-Lu is also breaking the time-reversal symmetry (this still waits confirmation). Magnetoresistivity and AC/DC susceptibility measurements allowed us to determine H_{c1} and H_{c2} of these films, as well as estimate coherence length $\xi(0)$ and magnetic penetration depth $\lambda_L(0)$. We also provide information on surface morphology of these films.

Keywords: superconducting films, rhenium, lutetium crystal structure, magnetoresistance, critical temperature, lattice parameters

I. INTRODUCTION

Non-centrosymmetric superconductors (NCS) with broken time-reversal symmetry (TRS) are of great interest to contemporary “hot topics” in superconductivity. Namely, these materials [1–3] provide the unique opportunity to design simple and scalable superconducting devices with nonreciprocal current control, such as diodes, transistors, quadrators, etc. [4–11]. Application of these materials inherently breaking NCS and TRS may abandon the necessity of external magnetic fields and sophisticated nano-patterning (such as reported in [12]). In Re-based compounds, such as Re-Nb [13], Re-Ti [14], Re-Hf [15] and Re-Zr [16], muon spectroscopy revealed broken time-reversal symmetry, complementing their non-centrosymmetric origin. This adds momentum to substantial interest in liquid-helium temperature superconductors which can be used in quantum information and computation technologies [17–19]. These thin-film superconductors can be easily deposited, and they are resistant to oxidation, have low resistivity, and/or are compatible with high magnetic fields [20, 21].

Rhenium itself belongs to transition metals, and in bulk form at ambient conditions, it superconducts below $T_c \approx 1.7$ K [22–24]. In a thin film form T_c is higher [22, 25–28] and can reach values as high as 6 K. Compounds of Re with other transition metals allowed material scientists to achieve not only higher values of T_c , but also, as was mentioned above to demonstrate broken TRS in addition to NCS. From this point of view it is interesting to explore superconductivity of Re-Lu substance, since there is a widespread opinion that the

lanthanide Lu is closer to transition metals than La itself [29]. However, Re-Lu material has not been explored in bulk form, or in thin films.

To close this gap, we report here on superconducting properties of amorphous and polycrystalline Re-Lu films with critical temperature up to about 7 K. We studied morphology of the films, magnetotransport and magnetic susceptibility which allowed us to estimate basic features of superconducting state, such as the critical fields, coherence length, and London penetration depth.

II. EXPERIMENTAL DETAILS

The Re-Lu films were prepared via magnetron sputtering in our ATC series UHV Hybrid deposition system (AJA International, Inc.) with a base pressure of 1×10^{-8} Torr. The Re target (ACI Alloys, Inc., 99.99% purity) was accommodated inside of a 1.5” DC gun. The Lu target (Heeger Materials, Inc., purity Lu/TREM 99.99%) was placed inside of a 2” DC gun. The sapphire substrate (AdValue Technology, thickness 650 μm , C-cut) was cleaned thoroughly with isopropyl alcohol before it was mounted on the holder. In our chamber’s configuration, the substrate holder is at the center of the chamber facing upwards, while the (five) sputtering guns are located at the top. The substrate is rotated in plane throughout the whole deposition process to ensure a homogeneous deposition layer over the whole surface. Our predeposition *in-situ* cleaning of the substrate typically involves heating it up to 900°C for 10 min followed by a gentle bombardment of Ar^+ ions at 600°C for 5-10 min using the Kauffman source at 45 degrees to the substrate surface. Then the temperature was raised to 900°C and kept at that value for 30 min. Afterwards, the temperature was reduced to 600°C and simultaneous deposition

* Corresponding author: gulian@chapman.edu

took place for 10 min, at pressure 3 - 4 mTorr, with gun power 250-260 W and anode voltage 605-460 V for Re, and with gun power 90-45 W and anode voltage correspondingly 325-275 V for Lu. Keeping the Re gun power constant, and varying the sputtering power of Lu from case to case allowed us to vary the values of x in composition Re_xLu (see Table I). After the deposition, the temperature was raised back to 900°C for in-situ annealing for 30 min and then cooled down to ambient temperature. All the heating/cooling protocols consistently used a 30°C/min ramp rate. The substrate was oriented to face the ion gun squarely.

III. RESULTS

Our initial choice of x for examining Re_xLu composition was $x \sim 4$, in analogy with the well-known NCS superconductor $\text{Re}_{0.82}\text{Nb}_{0.18}$, known for its breaking of TRS. The composition with $x \approx 3.8$ indeed turned out to be an amorphous superconductor with $T_c \approx 5.3$ K, see Fig. 1(a).

Lowering the relative concentration of the co-deposited Lu first increased and then decreased the T_c , with the optimum $T_c \approx 7$ K corresponding to $x \sim 10 - 11$ (shown also in Fig. 1). Though the normal state resistivities of these two compositions are not much different, they have very different surface morphologies, Fig. 2.

Comparative characteristics our films with various values of x are in Table I. To characterize the crystalline structure of our films we used grazing incidence X-ray diffractometry which excludes the reflections of the substrate. In this way it was recognized that the films with $x = 3.8$ are amorphous, and those with $x \approx 10$ are polycrystalline. In this report we will mainly focus on these two compositions. In the latter case, using the diffractogram (Fig. 3) it is possible to determine the lattice parameters of this novel substance. They are detailed in Table II. Magnetic and magnetotransport characterization of these films was also performed (Quantum Design PPMS), Fig. 4 and Fig. 5.

IV. DISCUSSION

As follows from Table I, both stoichiometric ratio and substrate's temperature affect the crystalline properties of this material. Moreover, the stoichiometric ratio itself depends on the substrate temperature. The last entry in the table corresponds to less than 1%(at.) of Lu in the composition - we reached here the resolution limit of our energy-dispersive spectrometer (Oxford Instruments X-Max^N). Meanwhile, as the special investigation revealed [28], pure Re films grown in the same conditions (600°C) are amorphous and do not superconduct down to 1.8 K, while being grown on 30°C they do at 3.6 K. The role of the substrate-film interplay is also important;

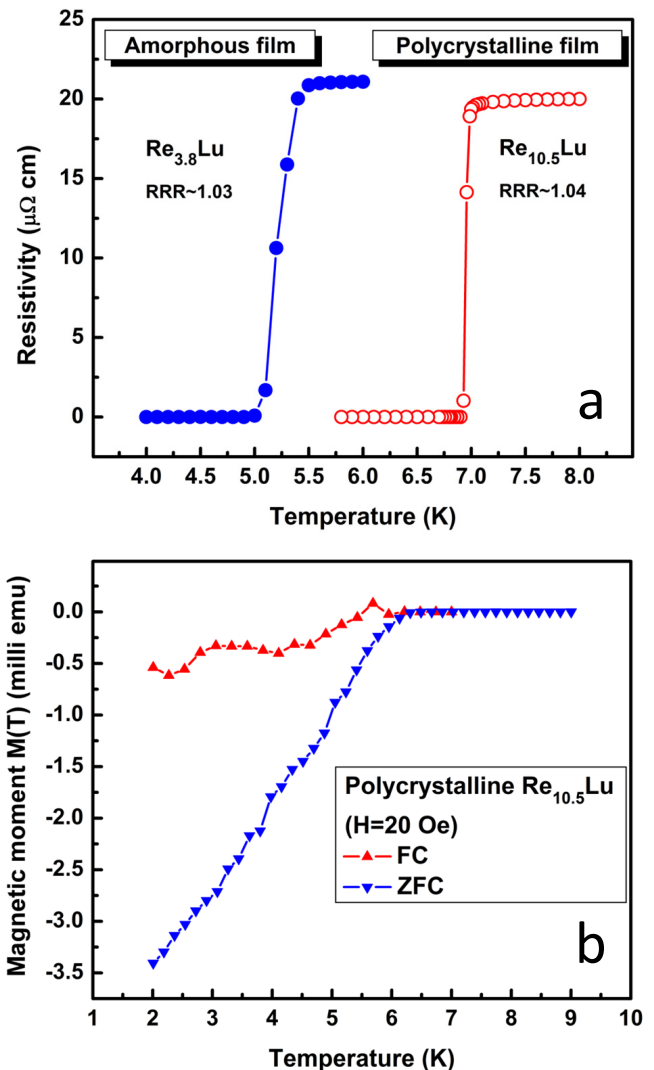


FIG. 1. (a) Resistive superconducting transition in amorphous (at $x = 3.8$) and polycrystalline (at $x = 10.5$) Re_xLu films (Quantum Design PPMS); (b) Meissner effect in polycrystalline $\text{Re}_{10.5}\text{Lu}$ film.

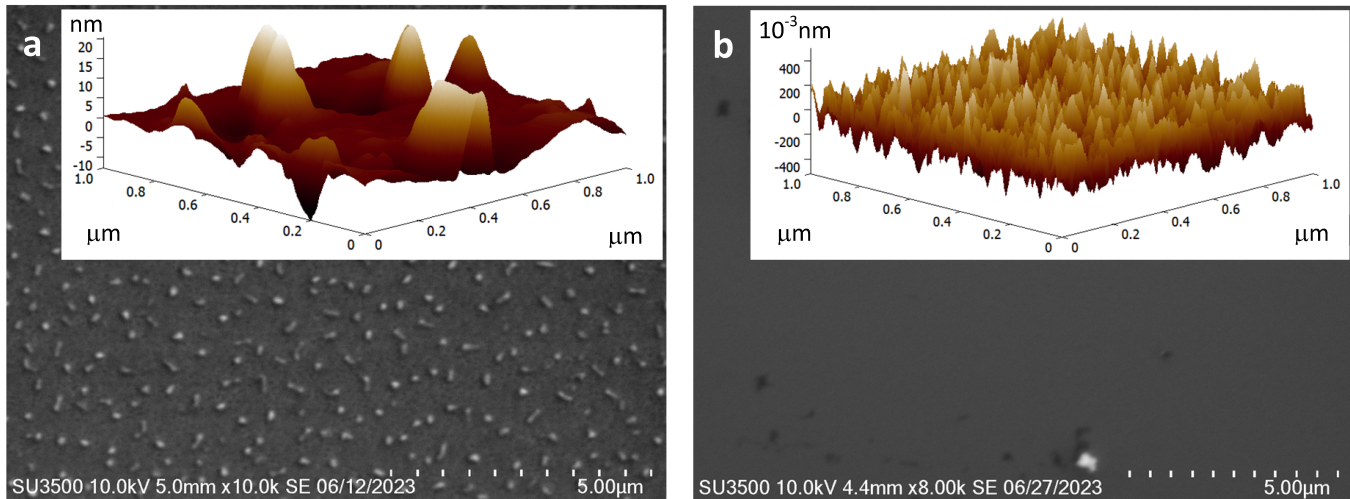
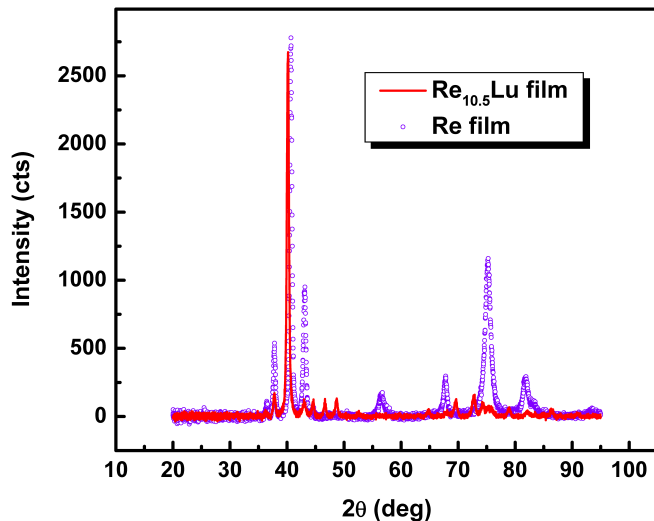
for example, bulk Re never superconducts above 1.8 K [22].

Our samples' H_{c2} (T) curves show different behavior compared to the conventional BCS dependence $H_{c2}(T) = H_{c2}(0)[1 - (T/T_c)^2]$. Therefore, the curves can instead be fitted using the expression $H_{c2}(T) = H_{c2}(0)[1 - (T/T_c)^p]^q$ following [30, 31] where the exponents $p = q$ were chosen to be 3/2. A slightly better fit to the data can be obtained when the constraint on p and q are removed by choosing $p = 1.8$, $q = 1.2$. This fit is shown in Fig. 5(b) which yields $H_{c2} \approx 13$ T. Using the Ginzburg-Landau relation $H_{c2} = \phi_0 / (2\pi\xi^2)$, where $\phi_0 = 2.068 \times 10^{-15}$ Wb is the flux quantum [32], the estimated coherence length of our film with $T_c = 6.95$ K is $\xi(0) = 5.05$ nm.

Combining $\xi(0)$ and the estimate for H_{c1} from panel (d) in Fig. 5 ($H_{c1} \sim 4$ Oe) [33] into the standard ex-

TABLE I. Re/Lu stoichiometry ratio, its T_c and the deposition parameters.

Re/Lu	P_{Lu} (W)	T_{substr} (°C)	Pressure (mTorr)	T_c (K)	Crystallinity
3.8	90	600	3	5.25	amorphous
7.4	55	30	4	6.1	amorphous
7.5	70	600	3	5.8	amorphous
10.5	55	600	3	6.95	polycrystalline
11.5	55	600	3	6.75	polycrystalline
>99	45	600	4	6.3	polycrystalline

FIG. 2. SEM (Hitachi SU3500) and AFM (insets, NT-MDT NTEGRA) characterization of surface morphology of the films with $x = 3.8$ (a) and $x = 10.5$ (b).FIG. 3. Grazing incidence X-ray diffraction pattern (Rigaku SmartLab) of polycrystalline $\text{Re}_{10.5}\text{Lu}$ film compared to that of pure Re film [28].

pression $H_{c1} = [\phi_0 / (4\pi\lambda_L^2)] [\ln(\lambda_L/\xi) + 0.12]$ [34], the estimate for our film's magnetic penetration depth is $\lambda_L(0) \approx 4.48$ nm. Finally, the Ginzburg-Landau parameter can also be calculated, $\kappa = \lambda_L/\xi = 0.89$, which shows that our film, being of type-II, is rather close to

the theoretical boundary separating type-I and type-II superconductors of $\kappa = 1/\sqrt{2} \approx 0.71$. This value of κ for polycrystalline $\text{Re}_{10.5}\text{Lu}$ matches with that obtained for pure Re films [28], though the individual values of λ_L and ξ are different.

For the amorphous $\text{Re}_{3.8}\text{Lu}$ with $T_c \approx 5.3$ K, the value of H_{c2} is a bit smaller: $H_{c2} \approx 11$ T (second curve in Fig. 5(b), obtained with the fitting parameters $p = 2.4$ and $q = 2.9$) yielding an estimate: $\xi = 5.5$ nm. From Fig. 4(c), $H_{c1}(T = 2.5\text{K}) \approx 3$ Oe. Taking into account that $H_{c1}(T = 5.3\text{K}) = 0$, one can use parabolic approximation used above and obtain an estimate $H_{c1}(0) \approx 3.88$ Oe [35]. This yields $\lambda_L(0) \approx 4.87$ nm and $\kappa = 0.89$, as in the case of polycrystalline films.

V. SUMMARY

Thus, the idea that Lu can successfully play the role of a transition element in Re–Lu compound is confirmed by this research. We obtained a new material, Re_xLu ($3.8 \leq x \leq 99+$). In particular, $\text{Re}_{10.5}\text{Lu}$ exceeds the critical temperature of known Re_6Hf , Re_6Zr and Re_6Ti . While these superconductors have never been reported having $T_c > 6$ K, either in bulk or thin film form, $\text{Re}_{10.5}\text{Lu}$ demonstrated $T_c \approx 7$ K. By analogy, one can expect that this NCS material will also break TRS. It will

TABLE II. Crystal structure comparison

Lattice parameters	$a, \text{Å}$	$b, \text{Å}$	$c, \text{Å}$	volume, Å^3	space group
Re, bulk [22–24]	2.761	2.761	4.458	29.430	P63/mmc
Re, film[28]	2.782	2.782	4.484	30.053	P63/mmc
Re _{10.5} Lu	9.6004(11)	9.6004(11)	9.6004(11)	884.86	217-43m

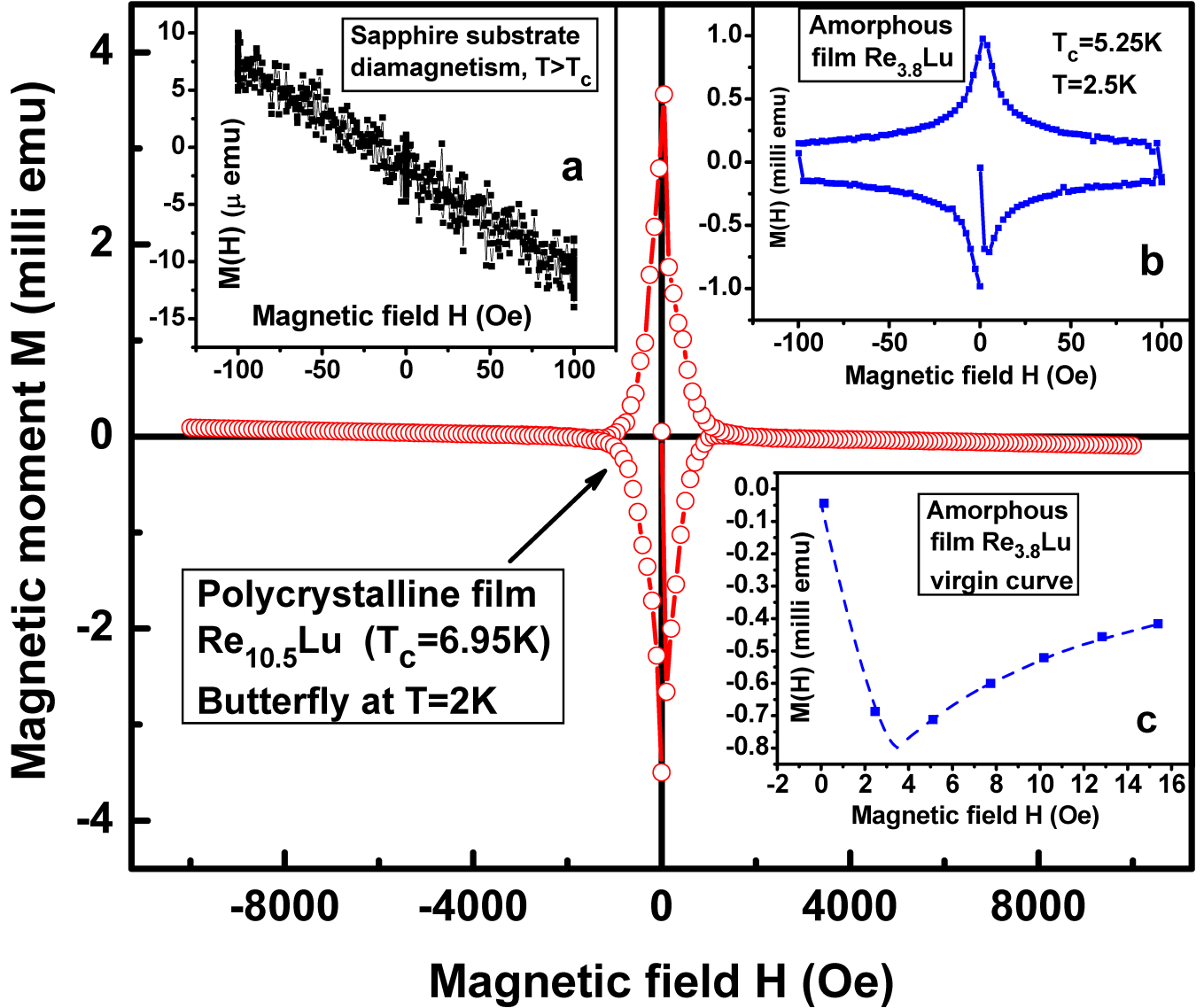


FIG. 4. Characteristic “butterfly” pattern of polycrystalline film $\text{Re}_{10.5}\text{Lu}$. A noticeable clockwise rotation of the butterfly is caused by the substrate diamagnetism (detailed in inset (a)). Inset (b) demonstrates the “butterfly” of $\text{Re}_{3.8}\text{Lu}$ amorphous film. Its virgin curve is shown in inset c (dashed lines are guides for eyes only).

be very interesting to explore that property, though that goal is beyond this paper. The indirect proof of broken TRS may be obtained by effects related to nonreciprocal current control devices made of this material: demonstration of nonreciprocity in absence of applied magnetic field may serve as such a proof.

The simplicity of the described deposition method may facilitate the application of this material for wide range

of devices mentioned in Introduction. Also, the information obtained by our research may provide grounds for further fundamental studies based on band-structure computations of superconducting state in Re-Lu materials to quantitatively explain the discovered features. Finally, the parameters λ_L and ξ estimated above may be used for modeling of phenomena in Re-Lu-based superconducting devices.

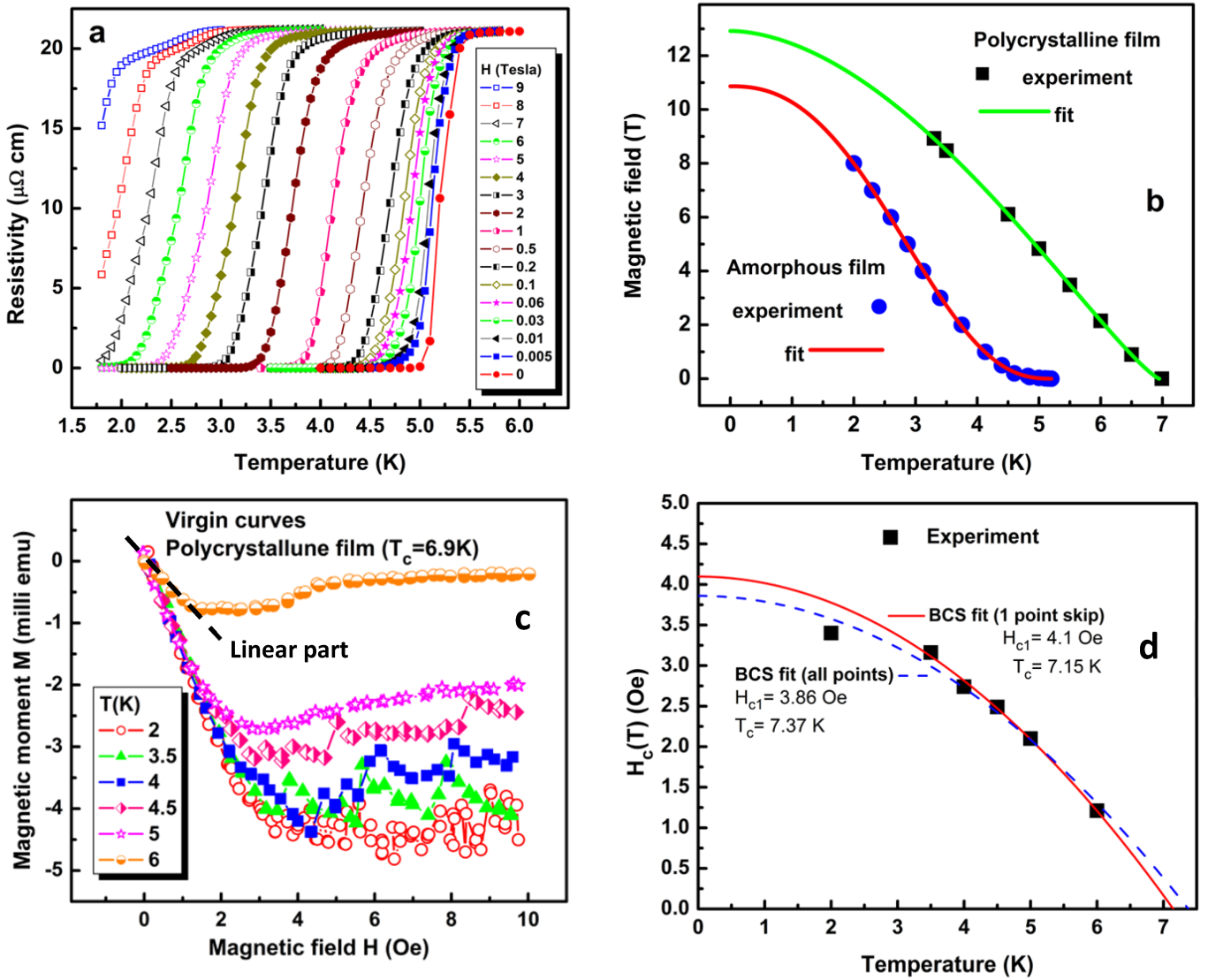


FIG. 5. (a) Magnetotransport measurements for determining critical field H_{c2} vs. temperature in case of $x = 3.8$ (amorphous) film. Similar measurements were performed in case of $x = 10.5$ (polycrystalline) film. (b) Determining $H_{c2}(T = 0)$ for polycrystalline and amorphous films. (c) Virgin curves of polycrystalline film at various temperatures for determining the value of H_{c1} (panel d). This value of H_{c1} is constructed in (d) using the linear part of experimental data (one such line is shown in panel c - dashed line for $T = 6 \text{ K}$ data) via modeling in accordance with the relation $H_{c1}(T) = H_{c1}(0)[1 - (T/T_c)^2]$.

ACKNOWLEDGMENTS

This research was supported by the ONR grants No. N00014-21-1-2879 and No. N00014-20-1-2442. We are grateful to Physics Art Frontiers for technical assistance.

- [1] Y. Tokura and N. Nagaosa, Nonreciprocal responses from non-centrosymmetric quantum materials, *Nature Communications* **9**, 3740 (2018).
 [2] R. Wakatsuki and N. Nagaosa, Nonreciprocal Current in Noncentrosymmetric Rashba Superconductors, *Phys.*

- Rev. Lett.* **121**, 026601 (2018).
 [3] S. Hoshino, R. Wakatsuki, K. Hamamoto, and N. Nagaosa, Nonreciprocal charge transport in two-dimensional noncentrosymmetric superconductors, *Phys. Rev. B* **98**, 054510 (2018).

- [4] F. Ando, Y. Miyasaka, T. Li, J. Ishizuka, T. Arakawa, Y. Shiota, T. Moriyama, Y. Yanase, and T. Ono, Observation of superconducting diode effect, *Nature* **584**, 373 (2020).
- [5] T. Ideue and Y. Iwasa, One-way supercurrent achieved in an electrically polar film, *Nature* **584**, 349 (2020).
- [6] C. Baumgartner, L. Fuchs, A. Costa, S. Reinhardt, S. Gronin, G. C. Gardner, T. Lindemann, M. J. Manfra, P. E. Faria Junior, D. Kochan, J. Fabian, N. Paradiso, and C. Strunk, Supercurrent rectification and magnetochiral effects in symmetric Josephson junctions, *Nature Nanotechnology* **17**, 39 (2022).
- [7] H. Wu, Y. Wang, Y. Xu, P. K. Sivakumar, C. Pasco, U. Filippozzi, S. S. P. Parkin, Y.-J. Zeng, T. McQueen, and M. N. Ali, The field-free Josephson diode in a van der Waals heterostructure, *Nature* **604**, 653 (2022).
- [8] E. Strambini, M. Spies, N. Ligato, S. Ilić, M. Rouco, C. González-Orellana, M. Ilyn, C. Rogero, F. S. Bergeret, J. S. Moodera, P. Virtanen, T. T. Heikkilä, and F. Giazotto, Superconducting spintronic tunnel diode, *Nature Communications* **13**, 2431 (2022).
- [9] T. Morimoto and N. Nagaosa, Nonreciprocal current from electron interactions in noncentrosymmetric crystals: roles of time reversal symmetry and dissipation, *Scientific Reports* **8**, 2973 (2018).
- [10] S. Chahid, S. Teknowijoyo, I. Mowgood, and A. Gulian, High-frequency diode effect in superconducting Nb₃Sn microbridges, *Phys. Rev. B* **107**, 054506 (2023).
- [11] S. Teknowijoyo, S. Chahid, and A. Gulian, Flux-Quanta Injection for Nonreciprocal Current Control in a Two-Dimensional Noncentrosymmetric Superconducting Structure, *Phys. Rev. Appl.* **20**, 014055 (2023).
- [12] Y.-Y. Lyu, J. Jiang, Y.-L. Wang, Z.-L. Xiao, S. Dong, Q.-H. Chen, M. V. Milošević, H. Wang, R. Divan, J. E. Pearson, P. Wu, F. M. Peeters, and W.-K. Kwok, Superconducting diode effect via conformal-mapped nanoholes, *Nature Communications* **12**, 2703 (2021).
- [13] T. Shang, M. Smidman, S. K. Ghosh, C. Baines, L. J. Chang, D. J. Gawryluk, J. A. T. Barker, R. P. Singh, D. M. Paul, G. Balakrishnan, E. Pomjakushina, M. Shi, M. Medarde, A. D. Hillier, H. Q. Yuan, J. Quintanilla, J. Mesot, and T. Shiroka, Time-Reversal Symmetry Breaking in Re-Based Superconductors, *Phys. Rev. Lett.* **121**, 257002 (2018).
- [14] D. Singh, S. K. P., J. A. T. Barker, D. M. Paul, A. D. Hillier, and R. P. Singh, Time-reversal symmetry breaking in the noncentrosymmetric superconductor Re₆Ti, *Phys. Rev. B* **97**, 100505 (2018).
- [15] D. Singh, A. D. Hillier, A. Thamizhavel, and R. P. Singh, Superconducting properties of the noncentrosymmetric superconductor Re₆Hf, *Phys. Rev. B* **94**, 054515 (2016).
- [16] F. N. Womack, D. P. Young, D. A. Browne, G. Catelani, J. Jiang, E. I. Meletis, and P. W. Adams, Extreme high-field superconductivity in thin Re films, *Phys. Rev. B* **103**, 024504 (2021).
- [17] T. M. Hazard, A. Gyenis, A. Di Paolo, A. T. Asfaw, S. A. Lyon, A. Blais, and A. A. Houck, Nanowire Superinductance Fluxonium Qubit, *Phys. Rev. Lett.* **122**, 010504 (2019).
- [18] L. Grünhaupt, M. Spiecker, D. Gusenkova, N. Maleeva, S. T. Skacel, I. Takmakov, F. Valenti, P. Winkel, H. Rotzinger, W. Wernsdorfer, A. V. Ustinov, and I. M. Pop, Granular aluminium as a superconducting material for high-impedance quantum circuits, *Nature Materials* **18**, 816 (2019).
- [19] D. Niepce, J. Burnett, and J. Bylander, High Kinetic Inductance NbN Nanowire Superinductors, *Phys. Rev. Appl.* **11**, 044014 (2019).
- [20] N. Samkharadze, A. Bruno, P. Scarlino, G. Zheng, D. P. DiVincenzo, L. DiCarlo, and L. M. K. Vandersypen, High-Kinetic-Inductance Superconducting Nanowire Resonators for Circuit QED in a Magnetic Field, *Phys. Rev. Appl.* **5**, 044004 (2016).
- [21] K. Borisov, D. Rieger, P. Winkel, F. Henriques, F. Valenti, A. Ionita, M. Wessbecher, M. Spiecker, D. Gusenkova, I. M. Pop, and W. Wernsdorfer, Superconducting granular aluminum resonators resilient to magnetic fields up to 1 Tesla, *Applied Physics Letters* **117**, 120502 (2020).
- [22] N. E. Alekseevskii, M. N. Mikheeva, and N. A. Tulina, The superconducting properties of rhenium, *Sov. Phys. JETP* **25**, 575 (1967), [*Zh. Eksp. Teor. Fiz.* 52, 875(1967)].
- [23] B. W. Roberts, Survey of superconductive materials and critical evaluation of selected properties, *Journal of Physical and Chemical Reference Data* **5**, 581 (1976).
- [24] C. Song, T. W. Heitmann, M. P. DeFeo, K. Yu, R. McDermott, M. Neeley, J. M. Martinis, and B. L. T. Plourde, Microwave response of vortices in superconducting thin films of Re and Al, *Phys. Rev. B* **79**, 174512 (2009).
- [25] A. Haq and O. Meyer, Electrical and superconducting properties of rhenium thin films, *Thin Solid Films* **94**, 119 (1982).
- [26] P. E. Frieberthausen and H. A. Notarys, Electrical Properties and Superconductivity of Rhenium and Molybdenum Films, *Journal of Vacuum Science and Technology* **7**, 485 (1970).
- [27] D. P. Pappas, D. E. David, R. E. Lake, M. Bal, R. B. Goldfarb, D. A. Hite, E. Kim, H.-S. Ku, J. L. Long, C. R. H. McRae, L. D. Pappas, A. Roshko, J. G. Wen, B. L. T. Plourde, I. Arslan, and X. Wu, Enhanced superconducting transition temperature in electroplated rhenium, *Applied Physics Letters* **112**, 182601 (2018).
- [28] S. Teknowijoyo and A. Gulian, Superconducting polycrystalline rhenium films deposited at room temperature, *Opt. Mem. Neur. Networks* **32** (2023).
- [29] E. Scerri, Mendeleev's Periodic Table Is Finally Completed and What To Do about Group 3?, *Chemistry International – Newsmagazine for IUPAC* **34**, 28 (2012).
- [30] P. K. Biswas, M. R. Lees, A. D. Hillier, R. I. Smith, W. G. Marshall, and D. M. Paul, Structure and superconductivity of two different phases of Re₃W, *Phys. Rev. B* **84**, 184529 (2011).
- [31] R. Micnas, J. Ranninger, and S. Robaszkiewicz, Superconductivity in narrow-band systems with local nonretarded attractive interactions, *Rev. Mod. Phys.* **62**, 113 (1990).
- [32] E. H. Brandt, Flux distribution and penetration depth measured by muon spin rotation in high- T_c superconductors, *Phys. Rev. B* **37**, 2349 (1988).
- [33] In this fitting procedure, the value of T_c is a free parameter. As follows from Fig. 5(d), its value is close to the experimental $T_c \approx 7$ K.
- [34] M. Tinkham, *Introduction to Superconductivity*, International series in pure and applied physics (McGraw-Hill, New York, 1975).
- [35] In this fitting procedure, the experimental value of T_c is

used, and the parabola is enforced to go through through 2 points: $H_{c1}(T_c) = 0$ and $H_{c1}(2.5\text{K}) \approx 3$ Oe. This

method is less accurate, however, it is satisfactory for estimates.